



**HAL**  
open science

# Effect of Slice Thickness on Texture-Based Classification of Liver Dynamic CT Scans

Dorota Duda, Marek Kretowski, Johanne Bezy-Wendling

► **To cite this version:**

Dorota Duda, Marek Kretowski, Johanne Bezy-Wendling. Effect of Slice Thickness on Texture-Based Classification of Liver Dynamic CT Scans. 12th International Conference on Information Systems and Industrial Management (CISIM), Sep 2013, Krakow, Poland. pp.96-107, 10.1007/978-3-642-40925-7\_10 . hal-01496055

**HAL Id: hal-01496055**

**<https://inria.hal.science/hal-01496055v1>**

Submitted on 27 Mar 2017

**HAL** is a multi-disciplinary open access archive for the deposit and dissemination of scientific research documents, whether they are published or not. The documents may come from teaching and research institutions in France or abroad, or from public or private research centers.

L'archive ouverte pluridisciplinaire **HAL**, est destinée au dépôt et à la diffusion de documents scientifiques de niveau recherche, publiés ou non, émanant des établissements d'enseignement et de recherche français ou étrangers, des laboratoires publics ou privés.



Distributed under a Creative Commons Attribution 4.0 International License

# Effect of Slice Thickness on Texture-Based Classification of Liver Dynamic CT Scans

Dorota Duda<sup>1</sup>, Marek Kretowski<sup>1</sup>, and Johanne Bezy-Wendling<sup>2,3</sup>

<sup>1</sup>Faculty of Computer Science, Bialystok University of Technology  
Wiejska 45a, 15-351 Bialystok, Poland

<sup>2</sup>INSERM, U1099, Rennes, F-35000, France

<sup>3</sup>University of Rennes 1, LTSI, Rennes, F-35000, France  
e-mail: {d.duda,m.kretowski}@pb.edu.pl

**Abstract.** This paper assesses the impact of slice thickness on texture parameters. Experiments are performed on liver dynamic CT scans, with two slice thicknesses. Three acquisition moments are considered: without contrast, in arterial and in portal phase. In total, 155 texture parameters, extracted with 9 methods, are tested. Classification of normal and cirrhotic liver is performed using a boosting algorithm. Experiments reveal that slice thickness does not considerably influence the stability of the parameters. They also enable to assess the rate of parameter dependency on slice thickness. Finally, they show that applying different slice thicknesses for training and testing the CAD system requires slice thickness-independent parameters.

**Keywords:** texture analysis, classification, dynamic CT, liver, slice thickness, stability of the parameters, tissue characterization, CAD.

## 1 Introduction

Various medical imaging techniques are available for acquiring a diagnostic information, e.g., Computed Tomography (CT), Positron Emission Tomography (PET), ultrasound, Medical Resonance Imaging (MRI), Single Photon Emission Computed Tomography (SPECT). With their rapid development, the image quality has been significantly improved. The images acquired over the years are characterized by increasing spatial and grey level resolution, and decreasing slice thickness. The number of images obtained within a single examination increases. The appropriate interpretation of an image information is thus a very complex task, but decisive for a correct diagnosis and treatment proposal.

Due to the fact, that the men are not able to identify such huge amount of information stored in the images, the (semi)automatic Computer Aided Diagnosis (CAD) systems become of a rapidly growing interest. Combining different image analysis techniques (like texture analysis [1] or segmentation) and classification algorithms, they appear to be a very promising diagnostic tool.

In most of the CAD systems based on imaging data two main stages of work can be distinguished. The first one, called *training*, is a preparation of the system

for the recognition of several classes of tissue, representing different pathologies. The second stage is the application of the system for the (semi)automatic recognition of new cases, not yet diagnosed. Due to the constant changes of image acquisition protocols, the question arises whether the protocols for new recognized images can be different from those that were used during the system training. The question seems all the more important given the fact that there is still no universal consensus on image acquisition protocols, so the images obtained from different machines could be of different properties and qualities.

The aim of our study is to examine the effect of slice thickness on texture parameters characterizing hepatic tissue on dynamic (contrast-enhanced) CT images. Our choice was dictated by the fact that the image database that we have been creating for about 10 years includes images of several slice thicknesses: from the oldest ones, of 10 mm, to the most recent ones, of 1.3 mm. So far, we have not found any research concerning the impact of slice thickness on texture-based classification of liver CT images with different contrast product concentrations.

In this study, we first assess the influence of slice thickness on parameter stability. Secondly, we study the possibility of tissue differentiation, with the most known parameters and different combinations of slice thicknesses used for system training and testing. Then, the parameter dependency on slice thickness is evaluated. Finally, the classification of two types of liver tissue, characterized by parameters which are least dependent on slice thickness is performed.

The next section includes a short description of related works. In Sect. 3 the system for classification of multiphasic textures is presented. Then, the methods for assessing the effect of slice thickness on the system performance are proposed. An experimental validation is described in Sect. 4. Conclusions and future work are presented in the last section.

## 2 Related Work

The effect of image acquisition protocols on CAD system performances has already been investigated in several studies.

In [2] the influence of slice thickness on CT-based texture parameters for cancellous calf bone was studied. Four different slice thicknesses were considered.

The work [3] analyzed the sensitivity of texture features of five different categories to variations in the number of acquisitions, repetition time, echo time, and sampling bandwidth at different spatial resolutions of T2-weighted MR images.

In [4] the effect of acquisition parameters, such as tube currents and voltages (10 different combinations), on texture was assessed on CT images of a cylindrical phantom filled with water. Eight different texture parameters were analyzed.

The effect of slice thickness on brain MRI texture classification was studied in [5]. In the work, thick slices were simulated on the basis of thin ones.

The first three of the cited studies showed that changes in all analyzed acquisition parameters could influence the texture parameter values, and thus – the texture discrimination. Only in the last work, the two considered tissue classes were separable even if slice thicknesses differed between training and testing sets.

### 3 Texture-Based Classification of Hepatic Tissues

#### 3.1 Two Stages of Work: Training and Aiding a Diagnosis

The system we develop for texture-based classification of multiphasic liver CT scans also works according to previously described two-stage model. Since typical CT exams of abdominal organs often consider three acquisition moments, which are related to the contrast product propagation in hepatic vessels, we proposed to analyze triplets of images [6], [7]. The first of the three simultaneously analyzed images corresponds to acquisition without a contrast. The second and the third are taken after its injection, at arterial and portal phases of contrast propagation.

The main steps of system training are shown in Fig. 1. First, a database of image triplets (preprocessed, if needed) is created. Then a Region of Interest (ROI) is drawn at the same position on each of the three corresponding images. Each ROI is characterized by the same vector of texture parameters. Three parameter vectors are thus created, each of them characterizes a texture at different acquisition moment. In the next step, parameters from those three vectors are concatenated, in order to make one "complex" parameter vector, describing a triplet of textures. The label representing a pathology is associated with each complex vector. At this moment, a set of labeled complex vectors could be subjected to a feature selection. Finally, it is used for the construction of the classifiers. Then the second stage of the system work can take place.

In order to recognize a new observation (see Fig. 2), a triplet of images is necessary. The three simultaneously analyzed images (in no contrast, arterial and portal phase) are subjected to the same preprocessing as it was in the training stage. Then three ROIs are drawn – one ROI on each of the three images. The triplet of ROIs is characterized in the same way as in the training stage. Finally, a complex vector of concatenated parameters (corresponding simultaneously to three acquisition moments) is classified. The tissue class that is attributed to this vector, is one of the classes considered in the training stage.

During the system design, many aspects must be investigated to ensure the best possible tissue recognition. One of them is the choice of the most relevant texture parameters. Such a choice must consider the variability of image acquisition settings that could result in different image properties, like those depending on slice thickness. Some ideas for adapting the system for working with images of different slice thicknesses are presented in the next part of our study.

#### 3.2 Parameter Stability

The estimation of parameter stability could help to decide if the parameter is reliable for proper tissue characterization. Parameters sensitive to small changes in ROI size, or small ROI displacements, should be excluded from further analyses.

We adopt the approach considered in [8] in order to assess how the parameter changes over the different ROI locations or sizes. As a measure of its changeability, the classical coefficient of variation (CV, the ratio of the standard deviation to the mean) is used. Stable parameters are characterized by low CV values, and

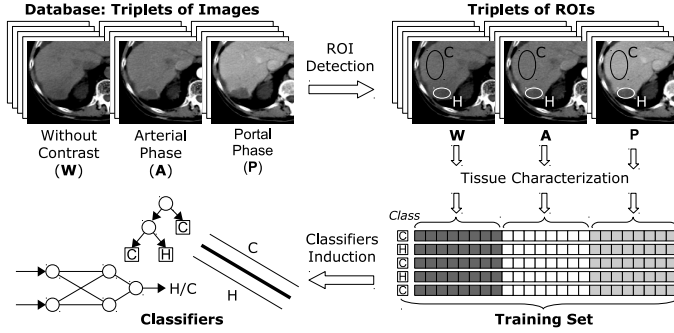


Fig. 1. System for texture-based classification of liver tissues: Training

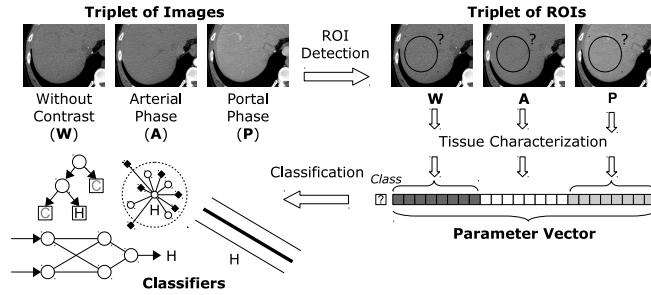


Fig. 2. System for texture-based classification of liver tissues: Aiding a diagnosis

the more unstable is the parameter, the greater is its CV. In our work, the CV of each texture parameter will be calculated for different slice thicknesses.

We propose to apply the following approaches: *Displace* and *Size Changing*. In the *Displace* approach, the initial ROI dimensions are first slightly decreased, then the reduced ROI is displaced in order to take all the possible positions inside its initial boundaries. On the basis of each new ROI location, the value of a parameter is calculated. With the *Size Changing* approach, the initial ROI size is successively reduced, pixel by pixel, by moving each time one of the subsequent ROI vertices. For each of thus obtained ROIs a parameter value is calculated. In both cases, a set of several parameter values, obtained for different ROI locations (*Displace*) or sizes (*Size Changing*) serves to calculate a CV.

### 3.3 Effect of Slice Thickness on Classification Accuracy

In order to evaluate the effect of slice thickness on the classification accuracy, we propose to perform several experiments, each time considering a different combination of slice thicknesses for training of classifier and for its test. If the image of a particular slice thickness is included in a training set, its counterpart (of the same slice position in a patient's body) of another slice thickness should not be included in the test set.

### 3.4 Effect of Slice Thickness on Parameter Values

To access the parameter dependency of the slice thickness, we propose a similar approach that we apply for the assessment of the parameter stability. For a given parameter, its dependency on slice thickness will be measured by a "variation" between several parameter values measured by the classical coefficient of variation. These values will be obtained for the same ROI position on images of the same acquisition moment, but characterized by different slice thicknesses.

In order to validate the usefulness of the slice thickness-independent parameters, the experiments on images with different slice thicknesses (different for a training and for a testing stage) will be performed.

## 4 Experiments

### 4.1 Database Description

The images, from 29 patients, were gathered at the Department of Radiology of the Pontchaillou University Hospital in Rennes, France. They were acquired with *LightSpeed16* device (*GE Medical Systems*). For each patient, three scan series were performed: without contrast, at arterial and at portal phase. The contrast material, of 100 ml, was injected at 4 ml/s, in an arm vein. The arterial phase acquisitions started about 20 seconds after the contrast product injection, the portal phase acquisitions started from 30 to 40 seconds later. For each of the three scan series, two "versions", corresponding to slice thicknesses of 5 mm and of 1.3 mm, were available. Each thick-slice image had its equivalent in thin-slice one, with the same slice position in the patient's body. All images had the size of 512×512 pixels. They were recorded in DICOM format, with 4096 gray levels. Since only the range of 248 gray levels sufficed for describing the pixels in the considered ROIs, the images were converted to a 8-bit BMP format.

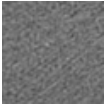
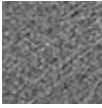
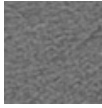
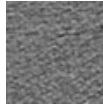

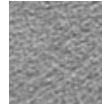
The 303 pairs of images (of a thick slice and of a corresponding thin slice) were taken into account for each of the three acquisition moments. Two classes of liver tissue were represented: cirrhotic and healthy liver (171 and 132 pairs of image triplets, respectively). A square ROI of 60×60 pixels was drawn at the same location on each of the 2·3=6 considered simultaneously images. An example of six corresponding ROIs is given in Table 1.

### 4.2 Texture Parameters Chosen for Evaluation

In total, 155 texture parameters, extracted with 9 methods, were tested (see Table 2). They are based on: First Order Statistics (FO), Gradients (GB), Co-Occurrence Matrices (COM) [9], Run Length Matrices (RLM) [10], Gray Level Difference Matrices (GLDM) [11], Laws Texture Energy (LTE) [12], Fractals (FB) [13], Texture Feature Numbers (TFN) [14], and Autocorrelation (AC) [15].

When applying the COM, GLDM, and RLM methods, the number of gray levels was reduced from 256, used initially, to 64. The CO Matrices and the GLD Matrices were constructed separately for 4 standard directions (0°, 45°, 90°, 135°).

**Table 1.** Six ROIs at the same slice position

Acquisition:	Without Contrast		Arterial Phase		Portal Phase	
ROI example:						
slice thickness:	5 mm	1.3 mm	5 mm	1.3 mm	5 mm	1.3 mm

135°) and for 5 different distances between the pixel pairs, going from 1 to 5. From each of 20 thus obtained matrices, the same parameters were calculated, 11 parameters by the COM method and 5 parameters by GLDM. The RL Matrices were also constructed for 4 standard directions, each of them served to calculate 8 parameters. For the three aforementioned methods, an averaging of the same parameter corresponding to 4 different directions was done. As the result, the following parameter sets were obtained: COM<sub>55</sub> (11·5 parameters), GLDM<sub>25</sub> (5·5 parameters), and RLM<sub>8</sub>. The sets COM<sub>11</sub> and GLDM<sub>5</sub> are the result of averaging of 20 parameter values, calculated for 4 directions and for 5 distances.

The normalized autocorrelation coefficients (AC) and the two TFN parameters (among 7) were calculated separately for 5 different pixel distances, from 1 to 5. They were included, respectively, in the sets AC<sub>5</sub>, and TFN<sub>15</sub> (with 5 other distance-independent TFN parameters). In the set TFN<sub>7</sub>, the values of 2 parameters calculated separately for the 5 distances were averaged.

The LTE method provided two parameter sets: LTE<sub>14</sub> and LTE<sub>5</sub>. The first one, composed of 14 parameters, was obtained by the application of 24 filtering masks of size 5×5: 4 symmetric, and 10 pairs of asymmetric ones, each pair consisted of a mask and its transposition. The second set was composed of 5 parameters, corresponding to the application of 3×3 masks, 2 symmetric and 3 pairs of asymmetric ones. The sum of elements of each convolution matrix was zero. For each pair of asymmetric masks, the resulting images were added. Images obtained by the application of symmetric masks were multiplied by two. Finally, the entropies of thus obtained images served as the texture parameters.

The FB method is based on the fractional Brownian motion model [16] and considers 4 pixel distances (1, 2, 3, 4). It provides a set of two parameters: FB<sub>2</sub>.

### 4.3 Effect of Slice Thickness on Parameter Stability

In this experiment, two approaches were applied for the CV calculation: *Displace* and *Size Changing*. The coefficient of variation was calculated on the basis of 9 parameter values. In the *Displace* approach, the ROI was reduced to a 58×58 square in order to take the 9 possible positions inside its initial boundaries. With the *Size Changing* one, the reduced ROI sizes were going from 60×60 to 52×52.

The experiment was performed separately for 12 texture sets, corresponding to all combinations of: 2 slice thicknesses, 2 tissue classes, 3 acquisition moments.

**Table 2.** Texture parameters chosen for evaluation. In bold – parameters which later turned out to be stable for both slice thicknesses

Set	Parameter Names
AC <sub>5</sub>	<b>(d)Autocorr</b> , where $d = 1, 2, 3, 4, 5$
COM <sub>55</sub>	<b>(d)InvDiffMom</b> , <b>(d)SumAvg</b> , <b>(d)SumEntr</b> , <b>(d)DiffEntr</b> , <b>(d)Entr</b> , <b>(d)AngSecMom</b> , <b>(d)SumVar</b> , <b>(d)DiffVar</b> , <b>(d)DiffAvg</b> , <b>(d)Contrast</b> , <b>(d)Corr</b> , where $d = 1, 2, 3, 4, 5$
COM <sub>11</sub>	<b>InvDiffMom</b> , <b>SumAvg</b> , <b>SumEntr</b> , <b>DiffEntr</b> , <b>Entr</b> , AngSecMom, SumVar, DiffVar, DiffAvg, Contrast, Corr
FB <sub>2</sub>	<b>FractalDim</b> , FractalArea
FO <sub>4</sub>	<b>Avg</b> , Var, Skewness, Kurtosis
GB <sub>4</sub>	<b>GradAvg</b> , GradVar, GradSkewness, GradKurtosis
GLDM <sub>25</sub>	<b>(d)DAvg</b> , <b>(d)DEntr</b> , <b>(d)DAngSecMom</b> , <b>(d)DInvDiffMom</b> , <b>(d)DContrast</b> , where $d = 1, 2, 3, 4, 5$
GLDM <sub>5</sub>	<b>DAvg</b> , <b>DEntr</b> , <b>DAngSecMom</b> , <b>DInvDiffMom</b> , <b>DContrast</b>
LTE <sub>14</sub>	<b>E5L5</b> , <b>S5L5</b> , <b>W5L5</b> , <b>R5L5</b> , <b>S5E5</b> , <b>W5E5</b> , <b>R5E5</b> , <b>W5S5</b> , <b>R5S5</b> , <b>R5W5</b> , <b>E5E5</b> , <b>S5S5</b> , <b>W5W5</b> , <b>R5R5</b>
LTE <sub>5</sub>	<b>E3L3</b> , <b>S3L3</b> , <b>S3E3</b> , <b>E3E3</b> , <b>S3S3</b>
RLM <sub>8</sub>	<b>ShortEmp</b> , <b>LongEmp</b> , <b>Fraction</b> , <b>HighGLREmp</b> , <b>REnter</b> , GLNonUni, RLNonUni, LowGLREmp
TFN <sub>15</sub>	<b>MeanConv</b> , <b>(d)CodeEntr</b> , Coarse, Hom, CodeVar, ResSim, <b>(d)CodeSim</b> , where $d = 1, 2, 3, 4, 5$
TFN <sub>7</sub>	<b>MeanConv</b> , <b>CodeEntr</b> , Coarse, Hom, CodeVar, ResSim, CodeSim

**Table 3.** Maximum parameter CV value (among 12 values, corresponding to: 2 approaches, 2 classes and 3 acquisition moments), obtained for 2 different slice thicknesses

Parameter	5 mm	1.3 mm	Parameter	5 mm	1.3 mm
(1)Autocorr	0.0004	0.0007	HighGLREmp	0.0035	0.0037
FractalDim	0.0012	0.0009	(4)CodeEntr	0.0036	0.0027
(5)SumAvg	0.0016	0.0017	S3E3	0.0038	0.0032
(1)SumAvg	0.0017	0.0018	(1)InvDiffMom	0.0039	0.0048
Avg	0.0018	0.0018	(3)AngSecMom	0.0047	0.0046
E3L3	0.0023	0.0021	GradAvg	0.0054	0.0052
DiffEntr	0.0026	0.0019	MeanConv	0.0058	0.0062
S5E5	0.0034	0.0031	DAvg	0.0063	0.0057

For each parameter, the CV values obtained from the same texture set were averaged. We observed that regardless of the approach, the three corresponding averaged CV values, obtained for three acquisition moments, did not differ sig-



nificantly. Nor did they differ between 2 tissue classes. The *Displace* approach almost always produced slightly higher CVs than the *Size Changing* approach.

Table 3 shows the averaged CV values obtained for the two different slice thicknesses. Each value is the maximum one of the  $2 \cdot 2 \cdot 3 = 12$  values, obtained for each combination of the approaches, classes and acquisition moments. Since the presentation of all the results occupies too much space, we present the results for 16 selected parameters. However, the CVs calculated on all 155 parameters yield the same conclusions as those obtained from the presented subset.

We can conclude, that the parameter stability, expressed by its coefficient of variation, is not considerably influenced by the slice thickness. Regardless of the extraction method, the CVs corresponding to thick and thin slices were similar. None of the thicknesses had proven to ensure better parameter stabilities.

For further experiments we decided to use the most stable parameters, for which the coefficient of variation does not exceed 0.01. The sets of parameters satisfying this condition were nearly identical for the two slice thicknesses. Only 4 parameters turned out relatively stable with only one of the thicknesses: CodeVar (rejected for thin slices, with  $CV=0.0102$ ), Contrast, DiffVar, and Hom (rejected for thick slices, with CV equal to 0.0144, 0.0195, and 0.1721, respectively). In total, 93 parameters were accepted for both slice thicknesses (see bolded parameters in Table 2), and the 62 parameters were rejected.

#### 4.4 Effect of Slice Thickness on Classification Accuracy

In this step, we considered the following combinations of slice thicknesses for training and for testing of the classifier:

- "T/T": training and testing performed on only thick slices (of 5 mm),
- "t/t": training and testing performed on only thin slices (of 1.3 mm),
- "T/t": training on only thick slices, testing on only thin slices,
- "t/T": training on only thin slices, testing on only thick slices,
- "mix": both thick and thin slices in a training and a testing set.

For each combination, the whole set of 303 pairs of image triplets (thick and thin version) was randomly divided into two subsets: a training set (202 pairs) and a testing set (101 pairs). For each subset, the original proportion between tissue classes was preserved. The experiment was repeated 10 times.

Table 4 presents the classification results obtained for the 5 combinations of slice thicknesses used for training and testing. Only the most efficient stable parameter sets are taken into account. Classification was performed with the Weka software [17], using Ensemble of Classifiers with adaptive boosting voting scheme [18] (*AdaBoostM1*) and a C4.5 tree [19] as the underlying algorithm.

We can observe that using the same slice thickness, both for training and for testing the classifier, results in a quite high classification accuracy. The best results are more frequent for thick slice thicknesses ("T/T" possibility). In this case, the maximal classification accuracy (86.73%) is obtained for the parameter sets  $COM_{55}$  and  $RLM_8$ . Just below the best results are those obtained when only

**Table 4.** Classification accuracy obtained by Ensemble of Classifiers for 5 combinations of slice thicknesses, used for training and testing. Each line corresponds to a different set of texture parameters. Only stable parameters are considered

Set	T/T	t/t	T/t	t/T	mix
COM <sub>55</sub>	86.73±2.48	84.75±2.73	63.07±2.24	56.64±5.52	78.72±4.81
COM <sub>11</sub>	84.16±3.33	82.97±3.29	64.16±2.08	53.77±5.57	77.13±4.26
GLDM <sub>25</sub>	67.03±2.47	69.81±6.40	56.84±1.76	48.02±2.61	57.93±1.94
GLDM <sub>4</sub>	63.47±3.51	61.09±4.55	56.94±0.70	49.21±6.32	56.84±0.96
LTE <sub>14</sub>	78.02±3.45	78.62±2.65	58.42±2.95	44.75±8.87	69.81±3.62
LTE <sub>5</sub>	74.46±3.67	74.46±4.89	59.71±7.61	49.50±4.48	63.27±5.25
RLM <sub>8</sub>	86.73±4.43	85.15±1.81	63.96±3.65	58.82±6.65	78.62±3.65

**Table 5.** Ranking of parameters by their dependency on the slice thickness

Rank	Parameter	Variation	Rank	Parameter	Variation
1	Avg	0.0024	21	(2)CodeEntr	0.0515
2	(5)SumAvg	0.0024	22	(3)CodeEntr	0.0515
3	(4)SumAvg	0.0024	23	RLEntr	0.0658
4	SumAvg	0.0024	24	E3E3	0.0750
5	(3)SumAvg	0.0024	25	E3L3	0.0787
6	(2)SumAvg	0.0024	26	E5E5	0.0803
7	(1)SumAvg	0.0025	27	S5S5	0.0811
8	FractalDim	0.0027	28	S5L5	0.0826
9	(1)Autocorr	0.0104	29	E5L5	0.0847
10	(4)Autocorr	0.0144	30	S5E5	0.0884
11	(5)Autocorr	0.0145	31	(1)SumEntr	0.0905
12	(3)Autocorr	0.0147	32	SumEntr	0.0931
13	(2)Autocorr	0.0155	33	(2)SumEntr	0.0932
14	HighGLREmp	0.0157	34	S3L3	0.0935
15	ShortEmp	0.0296	35	(3)SumEntr	0.0937
16	Fraction	0.0394	36	(4)SumEntr	0.0939
17	(1)CodeEntr	0.0511	37	W5E5	0.0941
18	CodeEntr	0.0514	38	(5)SumEntr	0.0945
19	(5)CodeEntr	0.0514	39	W5L5	0.0953
20	(4)CodeEntr	0.0515	40	S3E3	0.1016

thin slices are considered ("t/t"): 85.15% with the RLM<sub>8</sub> set. Slightly inferior results are observed when both slice thicknesses are considered for training and for testing ("mix"). The best of them is 78.72%, with the set COM<sub>55</sub>.

Unsatisfactory results are obtained when the slice thicknesses used for training and testing are different. Most of them do not exceed 60%. The best results for "T/t" and "t/T" combinations are: 64.16% and 58.82%, respectively.

We can conclude that, one should be careful using the system to aid the diagnosis, basing on images of a slice thickness different from those used for training.

However, we suppose that, in this case, the use of the texture parameters independent of the slice thickness could improve the system performance. The search for such parameters will be the subject of our next experiment.

#### 4.5 Effect of Slice Thickness on Parameter Values

In this experiment, we considered only those parameters that have been found to be stable for both slice thicknesses: 5 mm and 1.3 mm (see bolded parameters in Table 2). The parameter dependency from the slice thickness was expressed by the coefficient of variation of its two values, obtained from two corresponding ROIs (drawn on the images of a 5 mm and of a 1.3 mm slice thickness).

In total, 303 pairs of images were considered for each of 3 acquisition moments. For each parameter, the 3·303 values of the coefficient of variation were averaged. The ranking of parameters, according to the average coefficient of variation, was performed. Parameters with the lowest average coefficient are considered as least dependent on slice thickness. Table 5 presents the ranking of the first 40 parameters which are least dependent on the slice thickness.

Since we do not know how many parameters are acceptable and sufficient for the best possible tissue recognition, when different slice thicknesses are considered, we will test several sets of the first parameters from the ranking.

#### 4.6 Classification of Textures Characterized by Parameters the Least Dependent on Slice Thickness

In our final experiment, 7 parameter sets were tested: First-8, First-13, First-16, First-23, First-30, and First-39. They were composed, respectively, of the first 8, 13, 16, 23, 30, and 39 parameters from the ranking presented in Table 5. Table 6 presents the classification accuracy obtained for those 7 sets by Ensemble of Classifiers (with the same settings as in the previous classification experiment).

We can conclude that the classification accuracy, obtained for the 5 considered combinations of slice thicknesses are similar only when the First-8 parameter set is used. This set provides the classification accuracy ranging from 84.06%,

**Table 6.** Classification accuracy obtained by Ensemble of Classifiers for 5 combinations of slice thicknesses, used for training and testing. Each line corresponds to a different set of stable texture parameters, the least dependent of the slice thickness

Set	<b>T/T</b>	<b>t/t</b>	<b>T/t</b>	<b>t/T</b>	<b>mix</b>
First-8	85.94±4.12	86.64±2.77	85.35±4.78	84.06±4.08	87.13±3.90
First-13	87.43±2.64	87.53±1.76	67.03±3.59	75.94±3.62	82.58±3.10
First-16	87.82±2.84	87.63±3.17	63.47±2.11	73.96±6.42	85.05±3.21
First-23	89.51±3.50	88.42±2.76	62.38±3.10	74.46±4.82	86.24±3.38
First-30	91.39±3.10	88.52±6.00	64.06±2.92	71.09±5.00	88.22±2.49
First-39	90.79±3.93	92.48±2.10	62.78±1.88	66.74±6.78	88.32±2.71

for the "t/T" combination, to 87.13%, for the "mix" one. We can also notice that the application of the First-8 set guaranties the best classification results for the combinations, for which the slice thickness used for testing is different from that used for training (85.35% for "T/t" and 84.06% for "t/T"). For the first of these combinations, the best result is now 21.39% better than the best one obtained in the previous classification experiment, which did not consider the slice thickness-independent parameters (see Tab. 4). For the second one – the best classification accuracy augmented of 25.24%. Nevertheless, this accuracy still remain of about 6%-8% worse than the best results obtained now for the one-thickness cases ("T/T", "t/t").

In general, for the combinations "T/t" and "t/T", the more numerous is the set of parameters, the worse is the classification accuracy. Contrarily, for the one-thickness cases, the classification is generally better for more numerous sets.

With the "mix" combination, the application of the First-8 set leads to obtaining quite good classification accuracy, but not the best. In this case, increasing the number of parameters first results in lowering the classification accuracy (82.58% for the First-13 parameter set), then leads to its successive increase. Finally, the best classification result, for "mix" case (88.32%) is obtained by the most numerous parameter set, First-39, and is 9.60% better than the best accuracy observed, for "mix" case, in the previous classification experiment.

## 5 Conclusions and Future Work

The experiments allowed us to: (i) analyze the influence of the slice thickness on parameter stability, (ii) assess the parameter dependency on slice thickness, (iii) find parameters which are the least dependent on slice thickness, (iv) evaluate the classification accuracy obtained by parameters which are less and more dependent on slice thickness, when different slice thicknesses were simultaneously considered. Several conclusions can be formulated to sum up our study.

First, the parameter stability does not considerably depend on slice thickness. The sets of parameters recognized as stable were nearly identical for the two slice thicknesses. Second, one should be particularly careful when applying a CAD system, when recognized images are of the slice thickness different from the one used for the system training. With quite popular parameters, obtained by the COM or RLM methods, a satisfactory tissue recognition is not possible. In this case, it would be safer to use the slice thickness-independent parameters.

In the future, we plane to perform the experiments with more slice thicknesses. Due to the fact that acquiring the series of images of many different slice thicknesses is practically impossible within a single patient study, we plane to use a phantom. It will enable to assess not only the effect of the slice thickness in the texture-based classification, but also the effect of several other parameters, like image resolution, or the time elapsed from the contrast product injection.

**Acknowledgments** We thank Dr D. Olivie for his precious help. This work was supported by the grant S/WI/2/2013 from Bialystok University of Technology.

## References

1. Haralick, R.M.: Statistical and structural approaches to texture. *Proc. of the IEEE* 67(5), 786–804 (1979)
2. Guggenbuhl, P., Chappard, D., Garreau, M., Bansard, J.Y., Chales, G., Rolland, Y.: Reproducibility of CT-based bone texture parameters of cancellous calf bone samples: Influence of slice thickness. *Eur. J. Radiol.* 67(3), 514–520 (2008)
3. Mayerhoefer, M.E., Szomolanyi, P., Jirak, D., Materka, A., Trattnig, S.: Effects of MRI acquisition parameter variations and protocol heterogeneity on the results of texture analysis and pattern discrimination: an application-oriented study. *Med. Phys.* 36(4), 1236–43 (2009)
4. Miles, K.A., Ganeshan, B., Griffiths, M.R., Young, R.C., Chatwin, C.R.: Colorectal cancer: texture analysis of portal phase hepatic CT images as a potential marker of survival. *Radiology* 250(2), 444–452 (2009)
5. Savio, S.J., Harrison, L.C., Luukkaala, T., Heinonen, T., Dastidar, P., Soimakallio, S., Eskola, H.J.: Effect of slice thickness on brain magnetic resonance image texture analysis. *Biomed Eng Online* 9:60 (2010)
6. Duda, D., Kretowski, M., Bezy-Wendling, J.: Texture-based classification of hepatic primary tumors in multiphase CT. In: Barillot C., Haynor D.R., Hell P. (eds.) *MIC-CAI 2004, Part II. LNCS*, vol. 3217, pp. 1050–1051. Springer, Heidelberg (2004)
7. Duda, D., Kretowski, M., Bezy-Wendling, J.: Texture characterization for Hepatic Tumor Recognition in Multiphase CT. *Biocybern. Biomed. Eng.* 26(4), 15–24 (2006)
8. Lefebvre, F., Meunier, M., Thibault, F., Laugier, P., Berger, G.: Computerized ultrasound B-scan characterization of breast nodules. *Ultrasound Med. Biol.* 26(9), 1421–1428 (2000)
9. Haralick, R.M., Shanmugam, K., Dinstein, I.: Textural features for image classification. *IEEE Trans. Syst., Man Cybern.* 3(6), 610–621 (1973)
10. Galloway, M.M.: Texture analysis using gray level run lengths. *Comp. Graph. and Im. Proc.* 4(2), 172–179 (1975)
11. Weszka, J.S., Dyer, C.R., Rosenfeld, A.: A comparative study of texture measures for terrain classification. *IEEE Trans. Syst., Man Cybern.* 6(4), 269–285 (1976)
12. Laws, K.I.: Textured image segmentation. PhD thesis, University of Southern California (1980)
13. Chen, C., Daponte, J.S., Fox, M.D.: Fractal feature analysis and classification in medical imaging. *IEEE Trans. Med. Imag.* 8(2), 133–142 (1989)
14. Horng, M.H., Sun, Y.N., Lin, X.Z.: Texture feature coding method for classification of liver sonography. In: Buxton B., Cipolla R. (eds.) *Computer Vision – ECCV’96, Part I. LNCS*, vol. 1064, pp. 209–218. Springer, Heidelberg (1996)
15. Gonzalez, R.C., Woods, R.E.: *Digital Image Processing*, 2nd edition, Reading, MA: Addison-Wesley (2002)
16. Chen, E.L., Chung, P.C., Chen, C.L., Tsai, H.M., Chang, C.I.: An automatic diagnostic system for CT liver image classification. *IEEE Trans. Biomed. Eng.* 45(6), 783–794 (1998)
17. Hall, M., Frank, E., Holmes, G., Pfahringer, B., Reutemann, P., Witten, I.H.: The WEKA data mining software: an update. *SIGKDD Explorations* 11(1), 10–18 (2009)
18. Freund, Y., Shapire, R.: A decision-theoretic generalization of online learning and an application to boosting. *J. Comput. Syst. Sci.* 55(1), 119–139 (1997)
19. Quinlan, J.: *C4.5: Programs for Machine Learning*. Morgan Kaufmann, San Francisco (1993)